Journal of Materials Chemistry A

Accepted Manuscript

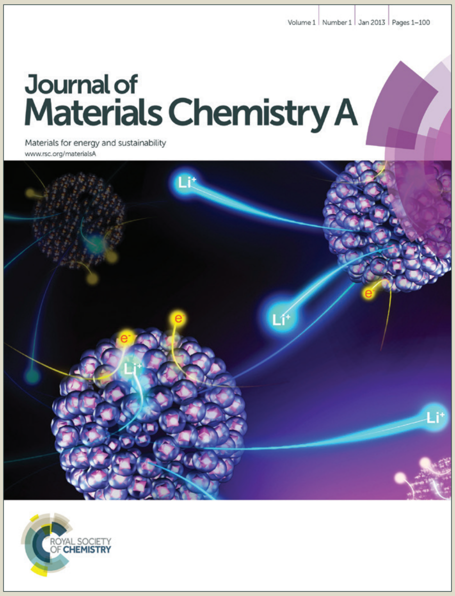

ROYAL SOCIETY OF CHEMISTRY

www.rsc.org/materialsA

Roughness-Controlled Copper Nanowires and Cu Nanowires-Ag Heterostructures: Synthesis and Their Enhanced Catalysis

Yang Sun[†, ‡], Fengying Zhang[†], Li Xu[†], Zhilei Yin[†] and Xinyu Song[*, †]

† School of Chemistry and Chemical Engineering, Shandong University, Jinan, 250100, P. R. China.

‡ Science and technology center, Qingdao water group co., Ltd, 250100, P. R. China.

Abstract

Effective surface and interface control of metal nanomaterials provides a powerful tool for realizing their enhanced catalytic properties. This article reports a remarkably simple approach for the preparation of copper nanowires with a rough surface. Surface roughness of Cu nanowires can be successfully controlled by adjusting the reactant ratio of the same kind of element ions with different valence state (Cu^+ and $Cu^{2+)}$. Furthermore, it is noted that as-prepared rough Cu nanowires have higher BET surface areas and a porous structure with a total pore volume of 4.212nm. Cu nanowires-Ag heterostructures are further prepared using the resulting rough Cu wires as “substrate”. Our experimental results reveal that Ag nanocrystals are preferentially grown on nanowires with a rough surface morohology compared to smooth nanowires. Due to surface effects and synergistic effect of their constituents, the as-prepared rough copper nanowires and Cu nanowires-Ag heterostructures demonstrated highly enhanced catalytic performance for the reduction of 4-nitrophenol. Especially, Cu nanowires-Ag heterostructures show superior catalytic activity compared with that of the obtained Cu nanowires with smooth surface, and recently reported some noble metal catalysts, such as pure Ag nanowires, magnetically Au nanocrystals,

---

[*] corresponding author E-mail: songxy@sdu.edu.cn

Au/grapheme hydrogel. This study offers a simple strategy that could be applied for the fabrication of other promising one dimensional Cu-based bimetallic nanometerials.

Keywords: copper nanowires, rough surface, Cu nanowires-Ag heterostructures, catalytic properties

1. Introduction

In the past decades, low-dimensional metal single-crystal nanostructure such as wires, rods and tubes have attracted an increasing amount of attention, because of their unusual properties and potential applications.[1-6] To date, a number of reports had been released to introduce synthesis of metal nanowires, such as Ag nanowires (NWs), Au NWs, Pt NWs, and Pd NWs. [7-10] Besides, these precious metals, copper NWs are attracting special interest due to their potential applications in the fields of optics, electronics, and SERS. [1, 11, 12] Many methods, such as template synthesis, [13] chemical vapor deposition (CVD),[14] electrochemical reactions,[15] and hydrothermal/ solvothermal reduction methods, [11] have been used for syntheses of the Cu NWs. However, most of these synthesis methods reported up to date are focused on producing Cu NWs with smooth surface, and little work has been made on the successful fabrication Cu NWs with rough surface morphologies. To the best of our knowledge, there are only two reports on the synthesis of Cu NWs with rough surface.[16,17] Cho* presented an electrodeposition technique to fabricate Cu NWs having various morphologies.[16] Recently, Chang et al. proposed a hydrothermal approach for producing hierarchical Cu NWs @RGO composites using catechin as the reducing agent and ethylenediamine (EDA) as the complexing agent.[17]

Copper nanocrystals are widely utilized as catalysts mainly due to its low-cost and higher abundance. Many studies have demonstrated that the catalytic activity depends not only on size and shape, but also on the surface microstructures or arrangement of the atoms on the surface. Effective surface and interface control over metal materials provides a powerful tool for realizing their enhanced catalytic properties.[18] Above all，surface morphology is a significant feature for NWs. The rough surface may greatly enhance the properties and performances of copper NWs, owning to a larger contact area, richer defect sites and more protrusions on uneven surface in comparison with smooth Cu NWs.[16,19] Moreover, compared to the ideally smooth surface, the rough surface may accommodate more deposited material leading to coatings of increased total surface area. Therefore, exploration of a simple and efficient method for the large-scale synthesis of roughness-controlled Cu NWs remains meaningful.

Nowadays bimetallic heterostructures have aroused extensive interest, because they are expected to display enhanced or new physical and chemical properties due to the synergy between the two metals in bimetallic heterostructural configuration.[20-23] Especially in catalysis, noble-nonnoble nanocrystals should be an ideal candidate of new low-cost catalysts with desired performance.[24] The cheap Cu nanocrystals, which possess good electronic transport and catalytic properties, can be an ideal substrate to form metal heterostructures with noble metal nanocrystals (e.g., Ag). However, so far, there is only one report on the successful preparation of wire-like Cu/Ag bimetallic composite using conventional chemical solution methods due to large lattice mismatch.[24] Moreover, in Ref. 24, Cu NWs-Ag Nanocrystals were prepared using relatively expensive raw materials in high temperature, which may be disadvantageous for practical application.

Herein, we report on the peculiar hydrothermal synthesis of the roughness-controlled Cu NWs in high yield by tuning the reactant ratio of the same kind of element ions with different valence state (Cu^+ and Cu^{2+}), using ascorbic acid as a reducing agent and cetyltrimethyl ammonium chloride (CTAC) as a structure directing agent. We demonstrate that the surface of the copper NWs from the smooth to the rough can be controlled by changing the reactant ratio between Cu^+ and Cu^{2+}. Then, we further synthesize Cu NWs-Ag heterostructures using the rough copper NWs as a platform through a partial galvanic replacement reaction between Ag and Cu. Our results demonstrate that an enlargement in the surface area of rough NWs “substrate” is favorable for deposing of Ag nanoparticles. The obtained copper

NWs with rough surface morphologies and Cu NWs-Ag nanocrystals show enhanced catalytic activity for the reduction of 4-nitrophenol to 4-aminophenol by $NaBH_4$ in aqueous solution compared with smooth copper NWs, as well as recently reported some precious metal catalysts. This as-developed synthetic system can be extended to fabricate other promising Cu NWs-based bimetallic materials.

2. Experimental

2.1. Materials

Cuprous chloride(CuCl), Copper chloride($CuCl_2$), cetyltrimethyl ammonium chloride (CTAC), ascorbic acid, silver nitrate ($AgNO_3$), poly(N-vinyl-2-pyrrolidone) (PVP), sodium borohydride ($NaBH_4$) p-nitrophenol (4-NP) were all analytical reagent grade and were directly used without further treatment.

2.2. Synthesis of Surface Roughness of Copper Nanowires and Cu Nanowire-Ag Nanocrystals

2.2.1 Synthesis of Roughness Surface Cu Nanowires

Roughness Copper NWs were synthesized by the following procedure. The mixture of 0.1 mmol (0.01g, therein copper about 0.064 g) CuCl solid and 1ml 0.01M (therein copper about 0.064 g) $CuCl_2$ solution was added into 25 mL of distilled water with magnetic stirring (mass ratio, Cu^{2+}: Cu^{+}=1:1), then 0.5 mmol (0.088 g) ascorbic acid and 0.01 mmol (0.032 g) cetyltrimethyl ammonium chloride (CTAC) were added to the above solution, and dissolved completely under stirring 10 mins. Finally, 0.5 mL NaOH (1 M) was rapidly dropped into the above mixture. After being vigorously stirred for 10 min, the mixture was later transferred to a Teflon-lined stainless steel autoclave sealed, and kept at 120°C for 2 h in a furnace and then cooled to the room temperature. The products were collected and washed with distilled water and ethanol, then dried in a vacuum oven at 50 °C for 8 h.

In addition, for comparison, smooth Cu nanowires were synthesized by using pure CuCl (0.015 g) as Cu source.

2.2.2 **Cu Nanowire-Ag Nanocrystals**

0.5 mL 0.01 M $AgNO_3$ solution was added dropwise into two beakers that contain 10 mL aqueous solution with rough-surface Cu NWs samples (about 8 mg). Meanwhile, 0.03 g PVP are added to the solution with magnetic stirring to make Cu NWs samples disperse sufficiently in the solution and N2 is bubbled into the solution to remove O_2. After 5 minutes mixing under vigorous magnetic stirring, gray precipitates quickly form and have fallen to the bottom. Then, the products are centrifuged at speed of 4000 rpm for 8 min and washed with ethanol for several times, then dried under the same processing conditions of the copper NWs as-synthesized.

2.3. Characterization Technique

The products were characterized by X-ray powder diffraction (XRD) on a German Bruker D8 X-ray diffractometer with Ni filtered Cu Kα radiation (λ= 1.5418Å). Transmission electron microscopy (TEM) patters were carried out on a JEM-100CXII at an accelerating voltage of 100 kV. Scanning electron microscopy (SEM) analysis was carried out using a JEOL JSM 6700F microscope operated with a 100 kV scale acceleration voltage. High-resolution TEM (HRTEM) image was characterized by a JEOL 2100 transmission electron microscope. The UV-vis absorption spectra were measured with a Hitachi U-4100 spectrophotometer.

2.4. Numerical Simulations

Molecular dynamics (MD) simulations have been extensively used to explore structures and electronic properties of materials molecules and have also been proved to be a reasonable and reliable tool.[25,26] MD simulation in canonical (constant atom number, volume, and temperature, NVT) ensemble was carried out to further investigate the growth mechanisms of copper NWs in the presence of CTAC molecules. In our study, the simulation method and structural analysis are similar to Bai's and Lai's work.[27-29] In order to determine the interaction modes and to calculate the interaction energy for each copper-CTAC system, three models were considered with same numbers of atoms and vacuum thickness for each copper-CTAC system: a three-dimensional model that contains a certain amount of CTAC molecules on a Cu crystal surface; Cu crystal plane only, and CTAC molecules only. Firstly, the optimized CTAC molecules were introduced over a crystal plane of Cu (i.e., {100}, {110}, or {111}) via the introduction technique implemented in Materials Studio software, and then was simulated for adsorption on the corresponding copper crystal plane. After the simulation adsorption, further MD simulations were performed for 100 ps for each copper-CTAC system. Different interaction strength of the CTAC molecules with different crystal planes of Cu (i.e., {100}, {110}, and {111}) were determined. All simulations were carried out by using the Discover Module of Materials Studio 4.4, and the COMPASS force field was employed to calculate the interactions. All the systems were undergone to energy minimization for the structural optimization before MD simulation. The simulations with NVT last for 100 ps with a time step of 1 fs. The relevant simulation data were collected in the last 100 ps of the simulation trajectory for each system.

2.5. Catalytic Reduction of 4-Nitrophenol

To study the catalytic performance of the as-prepared different copper samples, the reduction of 4-nitrophenol with sodium borohydride was chosen in following way. 0.091 mg Cu NWs were dispersed in 1 mL of 4-nitrophenol aqueous solution (1 mM) as reactants at room temperature. Then a freshly prepared aqueous solution of NaBH4 (2 mL, 0.025 M) was added as reducing agent. The mixture was immediately transferred into a quartz cuvette and the absorption spectra were recorded every 1~2 mins. The progress of the reactions was monitored by using a UV vis-NIR spectrophotometer.

3. Results and Discussions

3.1 Roughed Copper Nanowires

Fig. 1a shows an X-ray diffraction (XRD) pattern of the copper NWs, where the three peaks are assigned to the diffractions from {111}, {200}, and {220} planes of fcc Cu

(JCPDS 65-9026). A TEM image and SEM images of the prepared samples are presented in Fig. 1b-d, respectively. The as-prepared Cu NWs show an average diameter of 100 nm and a length up to about 25±5 μm as measured from SEM images. The enlarged SEM image of the product further displays that surfaces of Cu NWs are very rough and have many protrusions form (Fig. 1d)

To examine the role of reactant ratio between Cu^+ and Cu^{2+} in the formation of Cu NWs with a rough surface morphology, a series of control experiments have been carried out under same other conditions. Firstly, when only employing CuCl as copper source, the TEM image reveals that the surface of Cu NWs is highly smooth (Fig. 2a). An average diameter of the smooth samples is about 55 nm, which is smaller than the rough ones and a length reaches several tens of micrometers that indicated by SEM and TEM (shown in Fig. S1b and Fig. S1c, ESI†). The typical powder XRD pattern is shown in Fig. S1a (ESI†). All the diffraction peaks can be indexed for the fcc Cu. Then, the reactant ratio between Cu^{2+} and Cu^+ is changed to 1:3 (Cu^{2+}: Cu^+=0.021 g: 0.064 g), the as-obtained Cu samples are still smooth NWs but a few small protuberances grow on the surface of Cu NWs (see in Fig. 2b). When continuously increasing Cu^{2+} of the reactant ratio to 1:2 (Cu^{2+}: Cu^+=0.032 g: 0.064 g), it can be seen that more Cu protuberances appear and make the as-prepared NWs rougher (Fig. 2c). On further increasing the reactant ratio to 1:1 (Cu^{2+}: Cu^+=0.064 g: 0.064 g), the obtained NWs exhibit a very rough morphology and small protuberances wrap entire nanowires as depicted in Fig. 2d. It also can be seen that rough Cu NWs relative to smooth wires has a wider diameter (～100 nm). These results demonstrate that the reactant ratio between Cu^+ and Cu^{2+} plays an important role in controlling the surface roughness of Cu NWs.

To further investigate the growth mechanism of the rough Cu NWs, we systematically studied rough copper NWs evolution with different time period (1 h, 1.5 h, 2 h). Fig. 3 shows the powder XRD pattern and TEM images of Cu products based on the time evolution. From characterization results after the reaction time about 1 h, we can see that most of the products are smooth NWs with an average diameter about 55nm, and only a small amount of copper NWs are embedded with some particles (Fig. 3a). The corresponding XRD pattern of the as-obtained sample in Figure 3a is a mixture of copper and a small amount of cuprous oxide. After heating for 1.5 h, the product mainly consisted of Cu but still a few Cu_2O. The corresponding TEM in Figure 3c clearly reveals that the majority of obtained products exhibit the rough surface morphology with reaction time extending. After 2 h hydrothermal reaction, the final product is Cu nanocrystals with a highly uniform rough surface and its average diameter is about 100 nm (Fig. 3). Our results indicates that surface roughness and the diameter of the obtained products gradually increase with increasing the reactant ratio of Cu^{2+} and Cu^{+} from 0 to 1:1.

Then we study the exact role of CTAC in this reaction. To decipher the effect of CTAC on the growth of Cu NWs, controlled experiments are performed in the presence of different amounts of CTAC, only employing pure CuCl as copper precursor. Firstly, we prepared copper products without CTAC under the typical conditions described in the experimental section. It is noteworthy that only irregular shape-like particles are obtained (Fig. S2 in the Supporting Information). Upon adding 0.008 g CTAC, the wire-like copper crystals are formed but also with some irregular copper nanoparticles (Fig. 4a). When the amount of CTAC is further increased from 0.016 g to 0.024 g, the samples with wire-like shape become more, and fewer nanoparticles exist, as shown in Fig. 4b and 4c. While further increasing the amount of CTAC to 0.032 g, smooth copper NWs with high yield and great uniformity are obtained (Fig. 4d). These results clearly suggest that CTAC is crucial to the formation of copper NWs. The structure information of these smooth Cu NWs is further investigated by HRTEM. Taken from the middle and the end position of copper NWs (Figure S1d and S1f in the Supporting Information), two sets of lattice fringes of 0.215 nm and 0.182 nm are observed, corresponding to the {111} and {200} planes of Cu, respectively, which could suggest that the growth of the nanowire is along the <110> direction.[12] Thermodynamically, crystal planes with lower surface energy are preferably exposed. For an fcc Cu structure, the {111} plane has the lowest surface energy and tends to be exposed on the crystal surface to minimize the total surface energy. However, the presence of large amounts of

CTAC could effectively stabilize {111} and {200} planes by selective adsorption.[12, 30-32] To further study the role of CTAC, the adsorption of CTAC molecules on Cu (111), Cu (110) and Cu (100) surfaces is investigated using MD simulation. The three models created from MD simulation to indicate the CTAC molecule adsorption on each of the copper surface are described in Section S1 and Figure S3 in the Supporting Information. The energies for the formed complexes (Cu-CTAC), Cu facets, CTAC molecules on each surface and the interaction energies between CTAC and Cu (110), Cu (100) and Cu (111) crystal planes were calculated following the equation in Section 1 in the Supporting Information from the optimized models and listed in Table 1. Clearly, the interaction energies follow this trend: Cu (111) ≈ Cu (100) >> Cu (110), indicating that CTAC prefers to absorb on the Cu (111) and Cu (100) crystal planes rather than the Cu (110) plane, make Cu nanocrystals growth along <110> directions, then further form wires.

Based on a series of the experimental data, a possible growth mechanism has been proposed to elucidate the formation of copper NWs with a rough surface morphology. According to the table of standard electrode potentials, the reduction potential E^0 for the redox pairs Cu^{2+}/Cu (0.34 V) should be lower than that of the Cu^+/Cu (0.521V), so Cu^{2+} ions in aqueous solution have better stability than Cu^+ ions, thus Cu^+ ions are firstly reduced during the reaction.[33] Cu^+ ions released from the CuCl are reduced into Cu atoms with ascorbic acid and further form Cu smooth NWs due to selective absorption of CTAC. As the reaction proceeds, Cu^{2+} ions are subsequently reduced to Cu atoms, which grow on the surface of Cu NWs, resulting in the rough surface. As a result, the uniform rough NWs are formed and a possible reaction process schematic illustration is shown in Scheme 1.

3.2 Cu Nanowire-Ag Heterostructure

Figure 5a shows XRD pattern of the Cu NWs-Ag composite. From the XRD pattern, we can see that the main elements in the obtained sample are Cu and Ag. The three diffraction peaks shown by the black rhombus correspond to {111}, {200}, and {220} planes of fcc Cu. While the other four peaks indicated by the triangle can be indexed to {111}, {200}, {220} and {311} planes of fcc Ag (JCPDS 65−8428). In comparison with the XRD standard cards, the location of the diffraction peaks for obtained Cu-Ag composites do not shift, indicating that the Cu NWs “substrate” and the formed Ag nanocrystals are phase independent, not alloyed.[24] The TEM and HRTEM images of the obtained composite with an average diameter about 160 nm are shown in Figure 5b-d. It can be seen that no “free” Ag particles exist. The HRTEM image of an individual Cu NWs-Ag heterostructure demonstrates that the Ag nanocrystals have effectively grown on Cu NWs “substrate” with rough surface by the galvanic replacement reaction at room temperature. The lattice fringe of Ag nanocrystals is observed about 0.239 nm, which can be indexed to {111} plane of fcc Ag. On the other hand, the Cu lattice fringe is also obvious about 0.21 nm, corresponding to the {111} plane of fcc Cu, further confirming that the obtained product is Cu -Ag heterostructures. The composition of the bimetallic nanostructure was further characterized by EDS elemental mapping. The two elements Ag (green color) and Cu (red color) were scanned as shown in the EDS mapping profile of Fig. S4. In contrast, Ag nanocrystals can’t grow on smooth Cu NWs “substrate” as well as rough ones under same conditions and some “free” amorphous Ag nanoparticles are observed (shown in Fig. S5). This result suggests that higher roughness surface “substrate” can enlarge surface area and provide many surface defects that facilitate the deposition of Ag nanopariticles and accommodate more materials.[16,34]

3.3 The Catalytic Properties

As we already know, 4-aminophenol (4-AP) is very available in numerous applications that include analgesic and antipyretic drugs, photographic developers, corrosion inhibitors and so on.[35] The catalytic properties of the as-fabricated samples are measured for the reduction of aromatic nitro to amino group by $NaBH_4$ that monitored by UV−vis spectroscopy at room temperature (298k).[36,37] Designed for simplicity, those as-prepared Cu products with smooth surface and roughness surface are designated as Cu-1, Cu-2, respectively. Copper-silver NWs and commercial Cu powder are named as CuAg-3 and Cu-4, respectively.

To investigate the catalytic property of the as-synthesized samples, the reduction of p-nitrophenol by sodium borohydride absorption spectra with different catalysts are monitored with the progress of the time and these results are exhibited in Fig. 6. Commonly, the 4-NP has an original absorption maximum at 317 nm, but after addition of freshly prepared $NaBH_4$ aqueous solution at room temperature, the absorption peak immediately shifts from 317 to 400 nm and the color transforms from light yellow to dark yellow. This change has been owing to the formation of 4-nitrophenolate ions in basic condition caused by $NaBH_4$.[38] Without catalyst, the maximum absorption peak remains unaltered (shown in Fig. 6a). This suggests that even an excessive concentration of sodium borohydride can't reduce 4-nitrophenolate ion completely in the absence of catalysis. However, after the addition of the as-prepared Cu-1 NWs (0.091 mg), the absorption peak of 4-NP at 400 nm successively decreased along with the increase of a new absorption peak at 300 nm, indicating the appearance of 4-AP in Fig. 6b.[38] Same experiment processes are executed with Cu-2 and CuAg-3 and absorption spectra are shown in Fig. 6c and 6d, respectively. Moreover, for comparison, commercial Cu powder (Fig. 6e) is utilized for this reduction reaction in the same condition as before. Clearly, this reduction reaction could not be completed in one hour and the dark yellow color didn't fade. Fig. 6f displays the correlation between depletion of the 400 nm peak and different time by measuring UV-vis absorption recorded (i.e., ln(C/C_0) *vs.* reduction time), suggesting that the reaction is a pseudo-first-order. The rate constants estimated from the plots are 0.178, 0.252, 0.402, and 0.007 min^{-1} (shown in Fig. S6) for Cu-1, Cu-2, CuAg-3 and Cu-4, respectively. The observed results clearly demonstrate the CuAg-3 and Cu-2 are more efficient catalysts than Cu-1. In particular, the as-prepared CuAg-3 has more significant catalytic performance. In addition to the shape effect, it is widely accepted that the larger surface area can increase the catalytic activity.[39] For further understanding that catalytic activity of Cu-2 is higher than Cu-1, the BET surface area of the as-prepared samples are measured and the corresponding data are presented in Fig. S7. The sample Cu-2 with a rough surface exhibits a BET surface area of 11.84 m^2/g and a total pore volume of 4.212 nm (Fig.

S8 in the Supporting Information). Clearly, the surface area of the sample Cu-2 is larger than that of the Cu-1 with a smooth surface (3.73 m^2/g, shown in Figure S7). Moreover, the surface area of roughness Cu NWs is also higher than those of Cu nanospheres and Cu nanorods (6.1 m^2/g and 1.5 m^2/g) reported in the literatures,[40] commercial Cu powder and commercial Cu sheets (2.1042 m^2/g and 0.0316 m^2/g),[39] part of Ag nanopowders (8.25 and 7.8 m^2/g).[41] It is close to Ag nanoparticles (12.5 m^2/g).[42]

In addition, as is well known, the catalytic activity is originally correlated with the proportion of surface atoms located on the corners and edges of the metal nanomaterials.[43] Cu NWs with rough surfaces have a higher fraction of edges and corners than those of smooth Cu NWs, which may further enhance catalytic efficiency. Beyond the above reasons, the enhanced catalytic activity on bimetallic Cu NWs-Ag heterostructures can be attributed to the presence of the junction and synergistic electric effect of the binary components.[24, 44] It is known that Cu has the higher electron chemical potential relative to Ag, while Ag has higher electron conductivity than Cu.[45] Studies indicate that a small variation in local electronic structure at the interface between Cu and Ag can contribute to enhance the catalytic activity relative to their monometal.[45,46]

What’s more, for purpose of meaningful comparing our result with some noble metal (Ag, Au) catalyst as reported in the literatures, the activity factor (K) was defined as the values of pseudo-first-order rate constants (k) over the total weight of the catalyst.[45] By analyzing the plot of the concentration of 4-NP versus time with CuAg-3 as catalyst in Fig. 6d, the K value was estimated to be 0.074 s^{-1} mg^{-1} for CuAg-3. The data reveal that CuAg-3 shows more enhanced performance in catalytic aspect than the previously reported many noble catalysts, such as Ag−Au NWs (1%~10%), pure Ag nanowires,[44] magnetically Au NCs,[39] Au/grapheme hydrogel,[47] and dendritic Ag/Au,[48] but much cheaper raw material (as listed in Table 2).

In order to research the reusability of the obtained catalysts，CuAg-3 is assigned as a representative for better catalyst performance. The reusability and durability for sample CuAg-3 are tested in the reduction of 4-NP for three cycles. After the reaction, the nanocatalysts from centrifuge in the reaction mixture are washed with ethanol, and achieve reutilization for the next run under the same conditions. Fig.7 shows that the efficiency of CuAg-3 for the reduction processes is durable in the following catalytic cycles, declaring that the Cu NWs-Ag nanocrystals possess high durability.

4. Conclusion

In summary, this work demonstrates that copper NWs with highly rough surface can be successfully fabricated by simply adjusting the reactant ratio between Cu^{2+} and Cu^{+}, and its probable mechanism has been proposed. Both of the control experimental and simulated results suggest that CTAC is very necessary to the formation of wire–like Cu. The reactant ratios between Cu^{+} and Cu^{2+} can further control the surface roughness of NWs due to the difference in the redox potential. Furthermore, copper NWs-silver nanocrystals can be well formed by galvanic displacement reaction, demonstrating that Cu NWs with roughness surface can be used as a “substrate” to fabricate bimetallic nanocomposites. Catalytic experiments towards the reduction of 4-NP reveal that the synthesized Cu NWs-Ag heterostructures exhibit superior catalytic activity due to the large surface area and synergistic effect of the binary components. Our method can be extended to fabricate other promising Cu NWs-based bimetallic materials

Acknowledgements

This work was supported by the ZR2013BM027.

Reference

1 J. L. Duan, T. W. Cornelius, J. Liu, S. Karim, H. J. Yao, O. Picht, M. Rauber, S. Muller and R. Neumann, *J. Phys. Chem. C,* 2009, **113**, 13583.

2 X. Jiang, H. Yu, A. B. Low Dimensional Silver Nanostructures: Synthesis, Growth Mechanism, Properties and Applications. *J. Nanosci. Nanotech.*, **2010**, 10, 7829.

3 S. Chen, S. V. Jenkins, T. Jing, Y. Zhu, and J. Chen, *J. Phys. Chem.* C, 2013, 117, 8924.

4 J. Liu, Y. C. Son, J. Cai, X. Shen, S. L. Suib and M. Aindow, *Chem. Mater.*, 2004, **16**, 276.

5 C. He, P. Zhang, Y. F. Zhu and Q. Jiang, *J. Phys. Chem. C*, 2008, **112**, 9045.

6 M. Adachi, Y. Murata, J. Takao, J. Jiu, M. Sakamoto and F. Wang, *J. Am. Chem. Soc.*, 2004, **126**, 14943.

7 S. Chang, K. Chen, Q. Hua, Y. Ma and W. Huang, *J. Phys. Chem. C*, 2011, **115**, 7979.

8 C. Wang, Y. Hu, C. M. Lieber and S. Sun, *J. Am. Chem. Soc.*, 2008, **130**, 8902.

9 B. Y. Xia, H. B. Wu, Y. Yan, X. W. Lou and X. Wang，*J. Am. Chem. Soc.*, **2013**, **135** , 9480.

10 J. Wang, Y. Chen, H. Liu, R. Li, and X. Sun, *Electrochem. Commun.,* 2010, **12**, 219.

11 A. R. Rathmell, S. M. Bergin, Y.L. Hua, Z. Y. Li and B. J. Wiley, *Adv. Mater.* 2010, **22**, 3558.

12 H. Yang, S.-Y. He and H.-Y. Tuan, *Langmuir*, 2014, **30**, 602.

13 T. Gao, G.W. Meng, J. Zhang, Y.W. Wang, C.H. Liang, J.C. Fan and L.D. Zhan, *Appl. Phys. A*, 2001, **73**, 251.

14 H. Choi and S. H. Park**,** *J. Am. Chem. Soc.*, 2004, **126**, 6248.

15 M. E. T. Molares, V. Buschmann, D. Dobrev, R. Neumann, R. Scholz, I. U. Schucher and J. Vetter, *Adv. Mater.*, 2001, **13**, 62.

16 S. Shin, B. Kim, K. Kim, B. Kong, H. Cho and H. Cho，*J. Mater. Chem.,* 2011, **21**, 17967.

17 A. P. Periasamy, J. F. Liu, H-M. Lin, and H. T. Chang, H-T., *J. Mater. Chem. A***,** 2013, **1**, 5973.

18 B. Wu and N. Zheng, *Nano Today*, 2013, **8**, 168.

19 C. Cui and S. H. Yu, *Acc. Chem. Res.*, 2013, **46,** 1427.

20 W. Zhao, L. Yang, Y. Yin and M. Jin, *J. Mater. Chem. A*, 2014, **2**, 902.

21 J.P.Wang, D. F.Thomas and A. C. Chen, *Chem. Commun.* 2008, 5010.

22 H. Wu, S. Mei, X. Cao, J. Zheng , M. Lin , J. Tang , F. Ren , Y. Du, Y. Pan

and H. Gu, *Nanotechnol*., 2014, 25, 195702.

23 W. Chen, R. Yu, L. Li, A. Wang, Q. Peng and Y. Li, *Angew. Chem.*, 2010, **122**, 2979

24 M. Han, S. Liu, L. Zhang, C. Zhang, W. Tu, Z. Dai and J. Bao, *Appl. Mater. Interfaces*, 2012, **4**, 6654.

25 X.Q. Zhang, E. Iype, S. V. Nedea, A. P. J. Jansen, B. M. Szyja, E. J. M. Hensen and R. A. Santen, *J. Phys. Chem*. C, 2014, 118, 6882.

26. X. Q. Zhang, H. Li, and K. M. Liew, *J. Appl. Phys*. 2007, **102**, 073709

27 X. Bai, Y. Gao, H. Liu and L. Zheng, *J. Phys. Chem. C,* 2009, **113,** 17730.

28 Y. Lai, W. Pan, D. Zhang and J. Zhan, *Nanoscale*, 2011, **3**, 2134.

29 Q. H. Zeng, X. C. Jiang, A. B. Yu and G. Q. Lu, *Nanotechnology*, 2007, **18**, 035708.

30 M. S. Jin, G. N. He, H. Zhang, J. Zeng, Z. X. Xie and Y. N. Xia, *Angew. Chem., Int. Ed.*, 2011, **50**, 10560.

31 D. Zhang, R. Wang, M. Wen, D. Weng, X. Cui, J. Sun, H. Li and Y. Lu, *J. Am. Chem. Soc.*2012, **134**, 14283.

32 Y. Xia, Y. Xiong, B. Lim and S. E. Skrabalak, *Angew. Chem., Int. Ed.*, 2009, **48**, 60.

33 S. Sun and Z. Yang, *Chem. Commun.*, 2014, DOI: 10.1039/C4CC00304G

34 E. Ortel, S. Sokolov and R. Kraehnert, *Microporous Mesoporous Mater.*, 2010, **127**, 17.

35 Y. Chang and D. Chen, *J. Hazard. Mater.*, 2009, **165**, 664.

36 Y. Fang and E. Wang, *Nanoscale,* 2013, **5**, 1843.

37 S. S. Kumar, C. S. Kumar, J. Mathiyarasu and K. L. Phani, *Langmuir*, 2007, **23**, 3401.

38 P. Zhang, Y. Sui, G. Xiao, Y. Wang, C. Wang, B. Liu, G. Zou and B. Zou, *J. Mater. Chem. A,* 2013, **1**, 1632.

39 S. Gao, X. Jia, J. Yang and X. Wei, *J. Mater. Chem.,* 2012, **22**, 21733.

40 A. K. Patra, A. Dutta and A. Bhaumik, *Catal. Commun.*, 2010, **11**, 651.

41 M. Turker, *Materials Science and Engineering: A*, 2004, **367**, 74.

42 Z. Liu, G. Ren, T. Zhang and Z. Yang, *Toxicology*, 2009, **264**, 179.

43 H. Zhang, M. Jin, Y. Xiong, B. Lim and Y. Xia, *Acc. Chem. Res.*, 2013, **46**, 1783.

44 H. Fu, X. Yang, X. Jiang and A. Yu, *Langmuir*, 2013, **29**, 7134.

45 X. Huang,Y. Li, H. Zhou, X. Zhong, X. Duan, and Y.u Huang, *Chem. Eur. J.* , 2012, 18, 9505.

46 H. Zarick, W. R. Erwin, J. Aufrecht, A. Coppola, B. R. Rogers, C. L. Pint and R. Bardhan, *J. Mater. Chem*. A, 2014, **2**, 7088.

47 J. Li, C. Liu and Y. Liu, *J. Mater. Chem.*, 2012, **22**, 8426.

48 J. Huang, S. Vongehr, S. Tang, H. Lu, J. Shen and X. Meng, *Langmuir*, 2009, **25**, 11890.

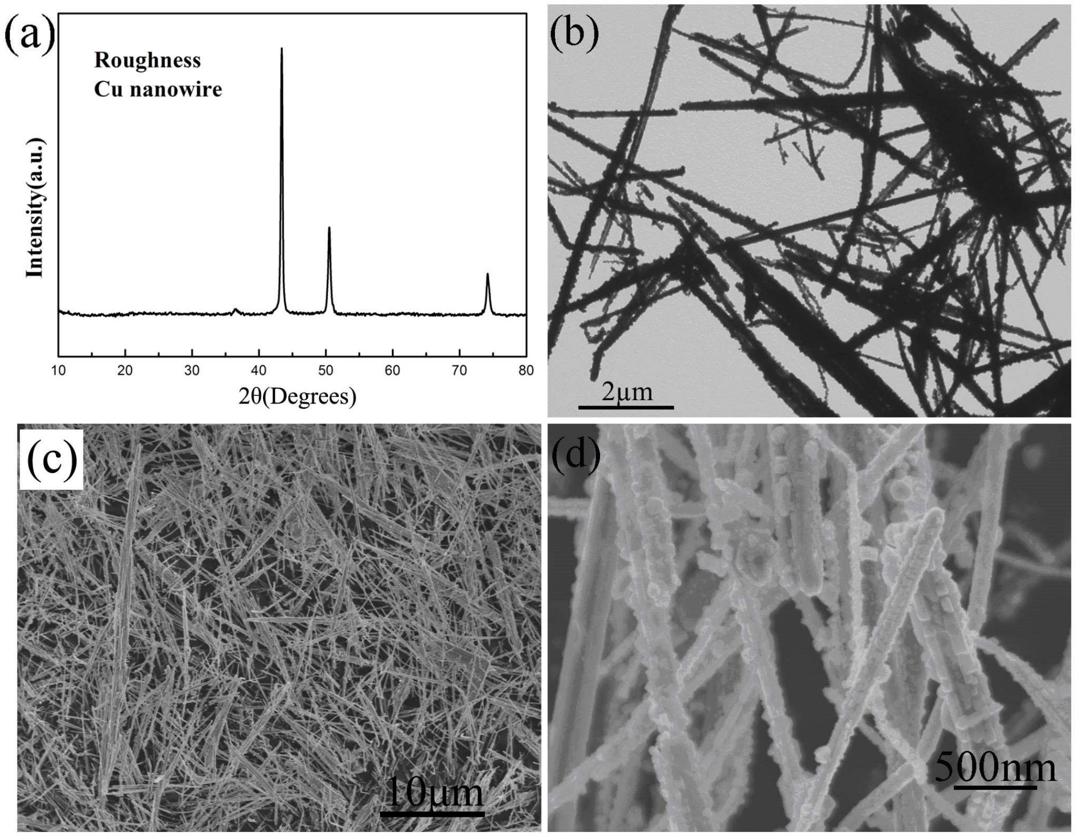

Fig. 1 (a) XRD pattern of the obtained copper NWs (b) TEM image of rough copper NWs. (c) Low- and (d) high-magnification SEM images of rough Cu NWs

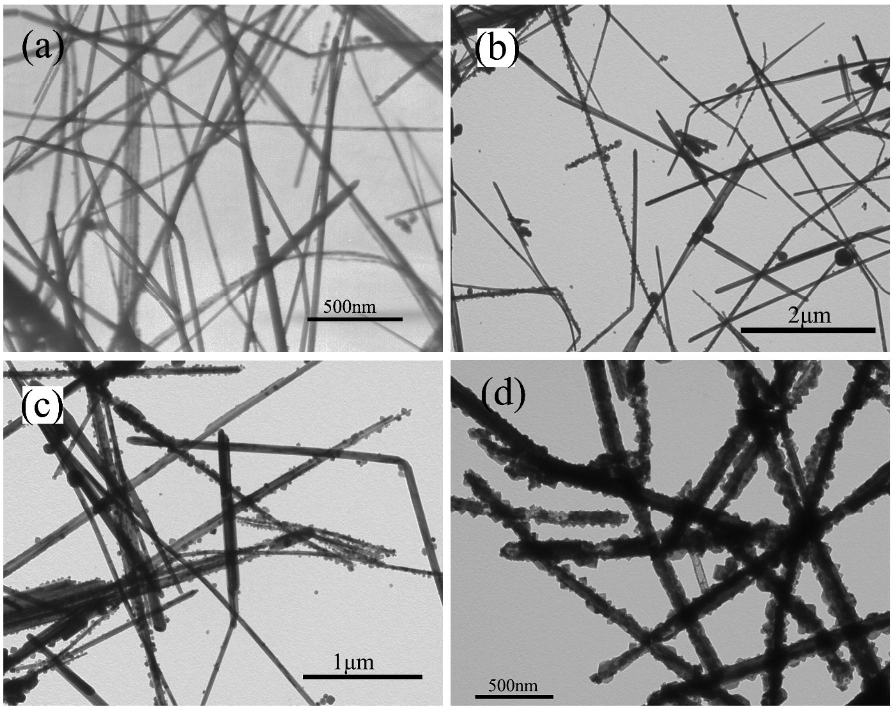

Fig. 2 TEM images of copper nanowires (from smooth to rough) sampled at different reactant ratio between Cu^{2+} and Cu^{+} (Cu^{2+}: Cu^{+}): (a) pure CuCl, (b) 1:3, (c) 1:2, (d) 1:1

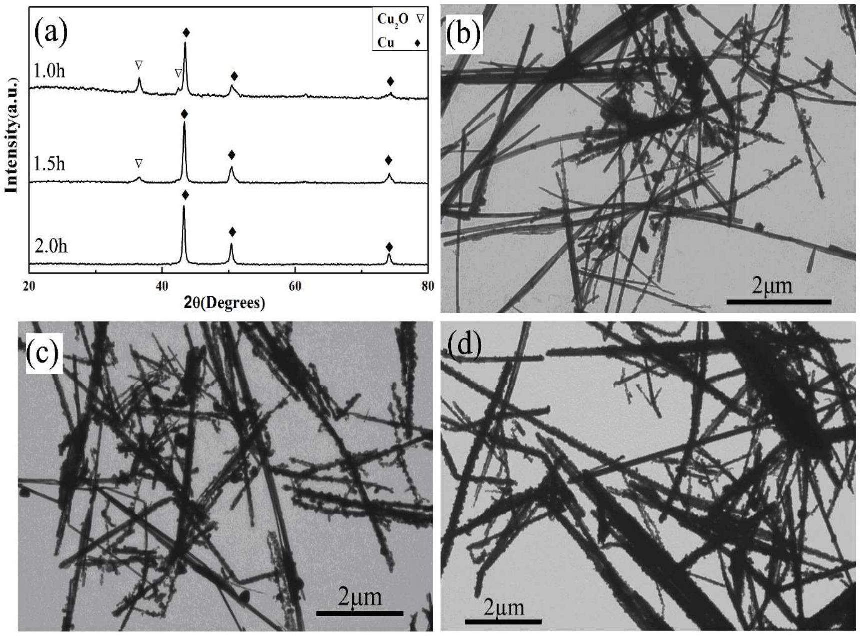

Fig. 3 (a) XRD patterns of the Cu samples obtained at different reaction stages. TEM images of the samples obtained at different reaction stages:（b）1.0h, (c) 1.5h, (d) 2.0h.

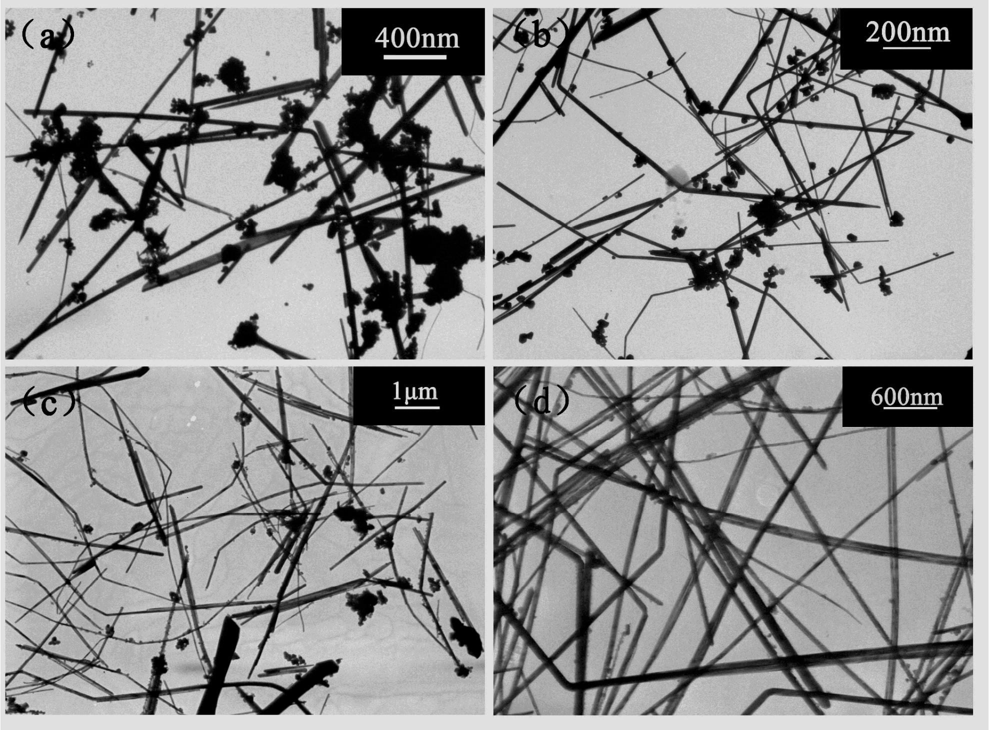

Fig. 4 TEM images of smooth copper NWs synthesized at 120°C for 2 h in a solution containing 0.064 g pure CuCl, 0.5 mmol ascorbic acid and different concentration of CTAC: (a) 0.008 g, (b) 0.016 g, (c) 0.024 g, (d) 0.032 g.

Table 1 Calculated interaction energies (kcal mol^{-1}) between CTAC and the various Cu crystal planes, a negative value mean an attractive interaction.

Plane	Cu(1 0 0)	Cu(1 1 0)	Cu (1 1 1)
E_{total}/kcal mol^{-1}	-16314.64	-14128.57	-16980.47
E_{CTAC}/kcal mol^{-1}	-71.75	-78.89	-77.79
E_{sur}/kcal mol^{-1}	-16072.47	-13948.06	-16723.93
E_{inter}/kcal mol^{-1}	-170.42	-101.62	-178.75

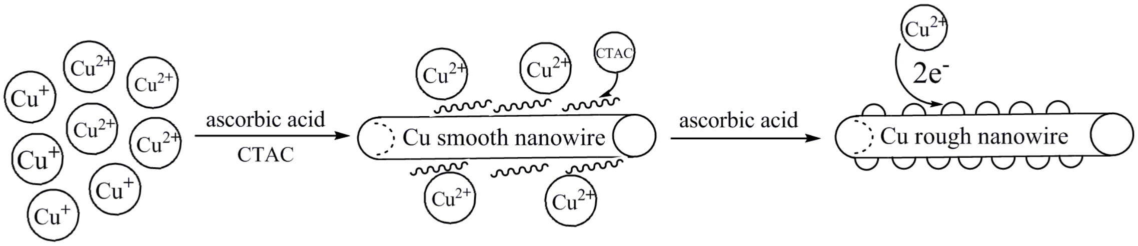

Scheme 1 Schematic illustration for the growth of Cu nanowires with a rough surface: Firstly, Cu^+ ions released from the CuCl are reduced into Cu atoms with ascorbic acid and further formed Cu smooth nanowires due to selective absorption of CTAC. Then, Cu^{2+} ions are subsequently reduced to Cu^0 and deposited on the surface of Cu NWs, resulting in the rough surface.

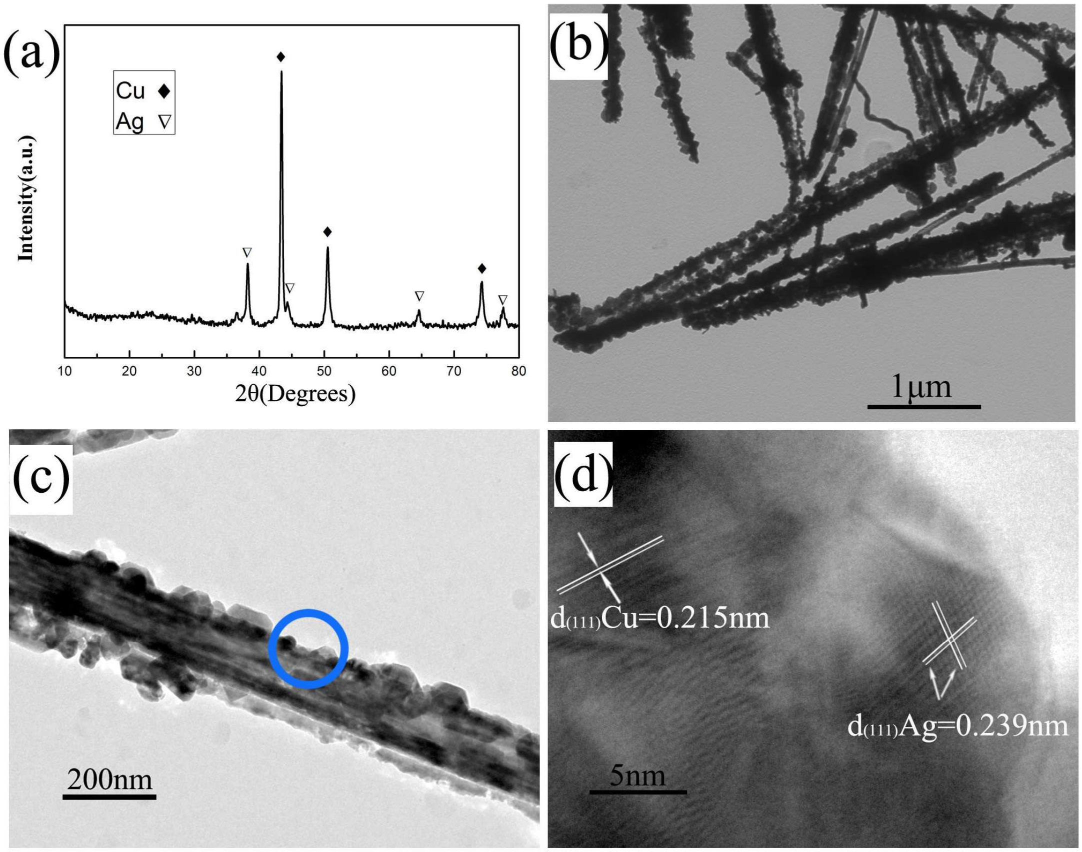

Fig.5 (a) XRD pattern of the obtained copper nanowires-silver nanocrystals. (b~c) TEM image of Cu NW-Ag . (d) HRTEM image of a rough surface Cu nanowire taken from blue circle in (c).

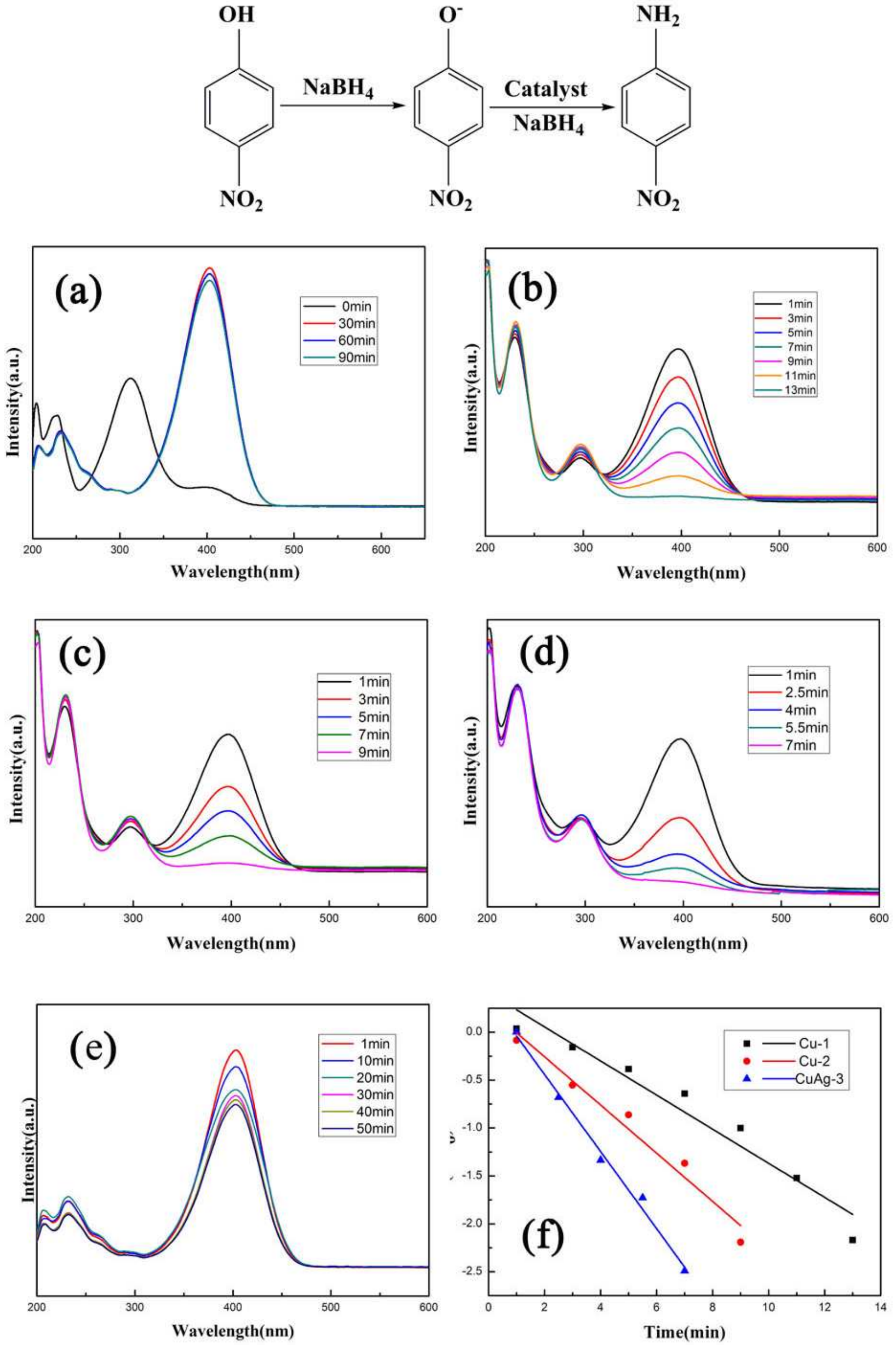

Fig. 6 Successive UV–Vis spectra of the reduction reaction. (a) in absence of any catalyst (b) Cu-1,(c) Cu-2, (d) CuAg-3, (e) Cu-4. (f) Absorbance ln(C/C_0) vs. time plot for the reduction of 4-NP in the presence of different solid catalysts (T=298K).

Table 2 Comparison of rate constants (k) and activity factor (K) of different catalysts for the reduction of 4-nitrophenol

Samples	**Quality/mg**	**Rate constant (k)/s^{-1}**	**Activity factor(K)/ s^{-1} mg^{-1}**	**Reference**
Cu NW-Ag (CuAg-3)	0.091	0.0067	0.074	This work
magnetically Au NCs	0.09	0.0052	0.058	31
Ag−Au Nanowires(10%)	0.0625	0.0038	0.061	40
Ag−Au Nanowires(5%)	0.0625	0.0034	0.054	40
Ag−Au Nanowires(1%)	0.0625	0.0014	0.022	40
Pure Ag nanowires	0.0625	0.0007	0.0112	40
Au/grapheme hydrogel	0.1	0.0031	0.031	43
Dendritic Ag/Au	0.6	0.0061	0.0101	44

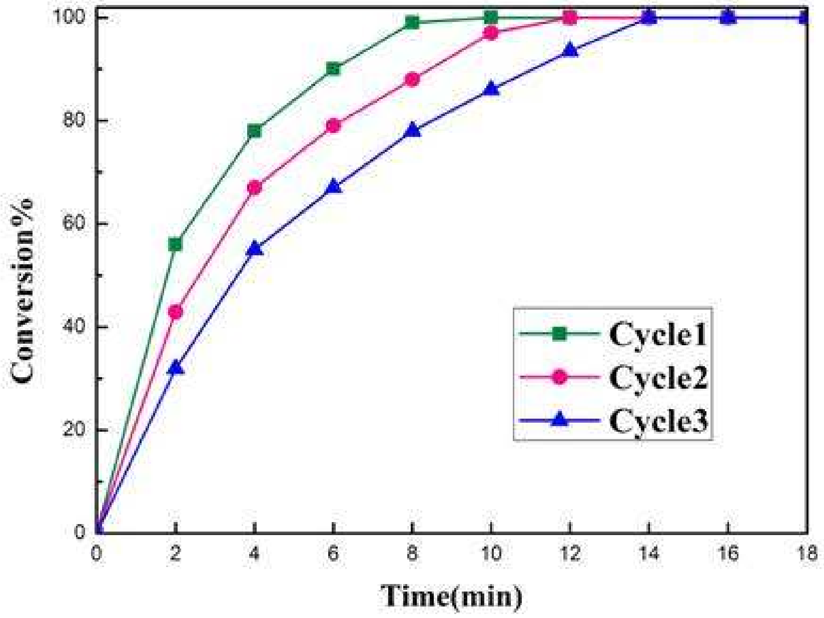

Fig. 7 Repeatability tests for 3 cycles of 4-NP reduction under the same reaction conditions over the Sample CuAg-3. Condition：[4-NP] = 1.0×10^{-3} M; Catalyst = 0.091mg; [$NaBH_4$] = 0.025 M; T = 298K.

Colour graphic:

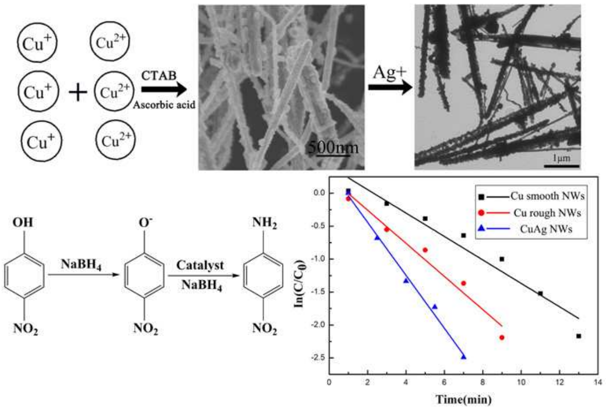

Cu nanowires-Ag heterostructures are prepared using the resulting rough Cu wires as “substrate”, which exhibit superior catalytic activity.